Temperature and Power Dependence of Photoluminescence in PbS Quantum Dots Nanoparticles
(Kesandaran Suhu dan Kuasa Pengujaan terhadap Fotoluminesens Titik Kuantum PbS Berzarah Nano)

Muhammad Safwan Zaini, Mazliana Ahmad Kamarudin*, Josephine Liew Ying Chyi, Shahrul Ainliah Alang Ahmad & Abdul Rahman Mohmad

ABSTRACT

In this study, the synthesis and the effect of temperature and power excitation towards photoluminescence (PL) emission of colloidal PbS quantum dots (QDs) were reported. Water soluble PbS QDs capped with a mixture of 1-thioglycerol (TGL) and dithioglycerol (DTG) was synthesized via colloidal chemistry method at room temperature. The PL emission of PbS QDs was investigated under temperature range from 10 K to 300 K and we found that the PL emission blue-shifted when the temperature is increased. From high resolution transmission electron microscopy (HRTEM), the average size of PbS core QDs is determined to be 6 nm and the integrated PL intensity (IPL) versus excitation power density shows the recombination of electrons and holes occur efficiently at low and high temperature for the PbS QDs. Full width half maximum (FWHM) shows a gradual broadening with the increasing temperature due to the interaction of charge carriers with phonons.

Keywords: Near infrared; PbS; photoluminescence; quantum dots

ABSTRAK

Dalam kajian ini, sintesis dan kesan terhadap suhu dan kuasa pengujaan fotoluminesens (PL) ke atas koloid PbS titik kuantum (QDs) dilaporkan. PbS QDs larut air ditutup dengan campuran ligan 1-tiogliserol (TGL) dan ditiogliserol (DTG) telah disintesis melalui kaedah koloid kimia pada suhu bilik. Pancaran PL daripada PbS QDs telah diuji pada julat suhu 10 K sehingga 300 K dan kami mendapati bahawa pancaran PL telah terjadi anjakan biru dengan peningkatan suhu. Daripada mikroskop elektron transmisi tinggi (HRTEM), purata saiz PbS QDs ialah sekitar 6 nm dan daripada data keamatan PL bersepadu (IPL) berlawanan ketumpatan kuasa pengujaan telah menunjukkan penggabungan semula eksiton berlaku secara cekap di dalam suhu rendah dan tinggi untuk PbS QDs. Lebar separuh ketinggian maksimum (FWHM) menunjukkan pelebaran beransur bersama peningkatan suhu disebabkan interaksi daripada pembawa cas dan juga fonon.

Kata kunci: Fotoluminesens; inframerah dekat; PbS; titik kuantum

INTRODUCTION

Colloidal quantum dots (QDs) have become one of the primary attention highlighted in current researched topic due to its unique intrinsic properties and potential used in optoelectronics and biomedical applications. Generally, QDs are semiconductor crystals with a size in the nanoscale region. It possesses a physical dimension that smaller than the exciton Bohr radius which lead to its excellent electronic properties based on the quantum confinement effect (Gao 2011). In this study, lead sulphide (PbS) QDs are selected because of its narrow bulk energy band gap at 0.41 eV and large exciton Bohr radius of 18 nm as compared to other materials such as CdS (2.8 nm) (Shamsudin & Junas 2018). It is worth mentioning that the effective mass of electron and holes in QDs are almost similar with $m_e^* \approx m_h^* \approx 0.08_0$, whereby m_0 is the electron mass in vacuum. This results eventually contributed to a strong confinement of both electrons and holes in the PbS QDs and benefit it potential in various optoelectronic application such as near infrared (NIR) photodetector, solar cell device, and light emitting diode (LED) (Guchhait 2011;

Iacovo 2016; Reilly 2014; Zhou et al. 2019). In addition, the size dependent optical absorption coefficient of QDs also allowed it to be used as a switchable device and ease the spectra modification in absorption, photoluminescence and electroluminescence spectra (Okamoto 2004).

Various methods have been conducted to synthesis a QDs such as molecular beam epitaxy (MBE), metal organic chemical vapour deposition (MOCVD), hydrothermal method and colloidal chemistry (Ashari et al. 2016; Tasco 2007; Yang et al. 2006; Yoffe 2001). It is noteworthy that a high crystalline QDs can be fabricated by MBE and MOCVD, however, it requires a high vacuum-technology equipment and high cost process. In contrast, the wet chemical colloidal approach provides a simple synthesis, feasible and low cost process (Yin & Alivisatos 2005). Also, it gives advantage to QDs because there is no need for QDs to be attached to a surface as they are prepared in solution. This can be used as nanometer size building blocks for interesting structures and electronic devices (Sargent 2005). Basically, the organic ligands were used during the colloidal technique, aiming to prevents the

agglomeration of PbS QDs due to the high surface free energy. Organic ligands also play a vital role in controlling the rate of kinetic growth of semiconductor crystal in a colloidal solution and indirectly stabilize the shape and dimension of QDs (Binetti et al. 2015; Rogach et al. 2007). Thus, the optimum selection of organic ligand is essential for surface functionalization, solubilization of ions during the preparation and modification of carrier confinements in QDs (Alivisatos 1996).

To understand the synergy relation between the localized states and carrier transport occurred in a PbS QDs based semiconductor material, temperature dependent photoluminescence spectroscopy is a common equipment used in the research. A study related to power excitation and temperature are introduced. There are many physical parameters that can be detected such as defects related to localized states, non-radiative processes, and carrier transport dynamics (Okamoto et al. 2004; Ryu et al. 2009; Szendrei et al. 2012; Yamada et al. 2009). Interestingly, the PbS QDs synthesized in this study present a high PL linewidth in the range of 150 meV to 170 meV when the operating temperature is increases from 10 K to 300 K. This results are outstanding as compared to previous report which detected at ~200 meV for PbS QDs embedded in glass (Peterson & Krauss 2006). It is strongly believed that the increases of excitation power density can bring forward to the modification the electronic and optical properties in QDs and acted as a new approach to study the mechanism behind the exciton-exciton interactions.

In this report, we report a study of the electronic and optical properties of PbS QDs prepared via colloidal synthesis. The characteristic of the emission spectra was evaluated in the function of temperature and power excitation from the temperature range of 10 K to 300 K. The PL study showed that the samples possess a near infrared (IR) emission at the range of 1000 nm to 1300 nm. The dependency between the full width at half maximum (FWHM) and integrated PL intensity (IPL) of the sample are also demonstrated.

EXPERIMENTAL SECTION

MATERIALS

1-thioglycerol (TGL, 95%), dithioglycerol (DTG, 95%) were obtained from Sigma Aldrich, lead (II) acetate trihydrate (99.99%), sodium sulphide nonahydrate (99.99%), were obtained from R&M Chemicals, triethylamine was purchased from Chemiz. The deionized water was used throughout the experiments with resistance of 18.2 MΩcm^{-1}. All chemicals were used as purchased.

SYNTHESIS OF COLLOIDAL PbS QDS

The synthesis of PbS QDs in aqueous solution was stabilised with capping ligands, namely, TGL and DTG. The molar ratio of Pb^{2+} and S^{2-} precursors is 1 and 0.3, respectively. During the synthesis of PbS QDs, lead acetate salt in solid crystal form was dissolved in deionized water and oxygen was removed from the system by flowing nitrogen gas. This oxygen-free environment avoids the oxidation of the QDs and sedimentation phenomenon (Wang et al. 2015). Meanwhile, 0.01 M solution of lead (II) acetate was prepared in a three-neck flask. 1 mL of the lead solution was added to the precursor beaker and the solution was allowed to mix for a few minutes. TGL and DTG were added into the three-neck flask containing lead precursor and magnetic stirrer running at 400 rpm. The solution then turned to yellowish green. These ligands (TGL and DTG) were added to avoid agglomerations. Triethylamine was added to the solution drop wise to adjust the pH until it reaches to pH10 and the solution turned colourless. After 15 min, 0.1 M solution of sodium sulphide was immediately introduced into the system, accompanied by continuous stirring. The solution changed from colourless to dark brown immediately, indicating the formation of lead sulphide QDs. All the samples were stored in the dark at low temperature (4°C).

CHARACTERIZATION

For optical measurements (PL spectroscopy), the 532 nm laser beam was used as an excitation source with the closed cycle He cryostat system measured temperature range from 10 K to 300 K as shown in Figure 1. The temperature controller was used to vary the temperature. The emitted PL was collected by a lens and then focused onto the entrance slit of the monochromator before being detected by an InGaAs detector. The integration time was 1 s and the investigated wavelength range from 800-1600 nm. For the sample preparation, the colloidal PbS QDs was drop casted on the glass substrate for PL measurement.

For high resolution field emission transmission electron microscope (HRTEM), the sample was prepared by drop-casting the small volume of the PbS QDs onto the Cu grid coated with an ultrathin coated film. The structural characterization was performed using FEI Tecnai-G2 20 S-TWIN TEM by Crest Group. The size distribution, pattern and particle size of QDs for the sample was characterized by HRTEM.

RESULTS AND DISCUSSION

COLLOIDAL SYNTHESIS

Figure 2 displays the colloidal PbS QDs synthesized in aqueous solution and capped with thiols ligands (TGL and DTG). These organic ligands have functional group of sulphur and hydrogen atom, which bind to the QDs surface with hydrogen bond. From Figure 2, the diagram shows the capping ligands preventing the PbS QDs from agglomeration by creating a protection to QDs from binding effect, where the area between QDs is covered by ligands, causing repulsion between QDs that stabilizes the colloid (Liu et al. 2018). Generally, long chain thiols are excellent capping ligand for most semiconducting and metal
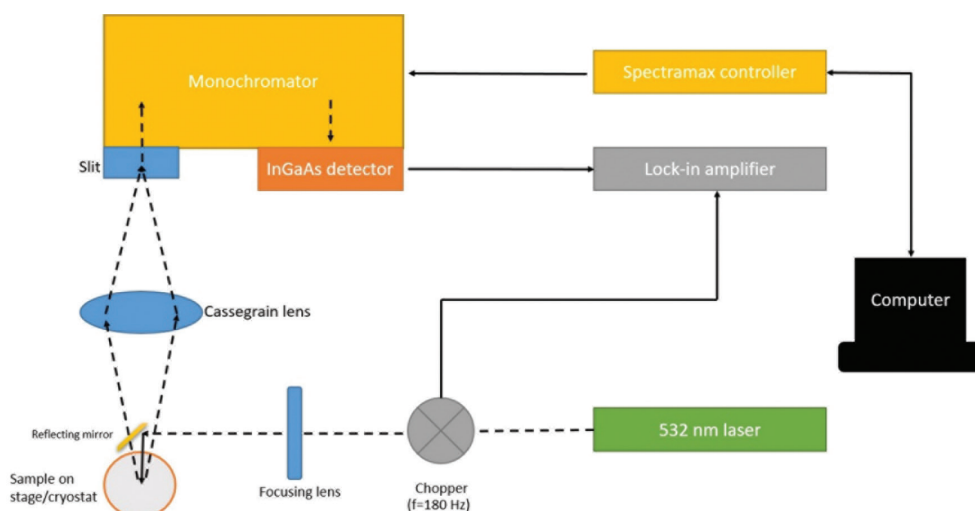
FIGURE 1. The schematic diagram of photoluminescence (PL) setup equipped
with cryostat system for temperature dependent measurement
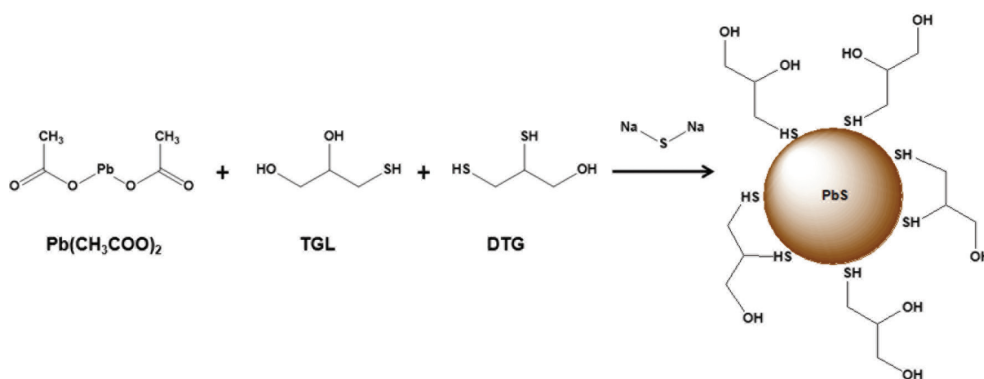

FIGURE 2. The schematic figure of the chemical reaction between PbS QDs with the ligands

nanoparticles. For instance, thiol stabilised colloidal CdTe QDs was firstly reported that led to the repetitive use of the ligands with QDs (Rajh et al. 1993). Unfortunately, this colloidal PbS QDs is highly sensitive to the environment and temperature. It was observed that the sample was agglomerated when exposed to ambient oxygen at relatively high temperature. Therefore, the colloidal PbS QDs was kept at low temperature to slow down the growing process of QDs, thus making the size of QDs smaller as well as preventing the formation of bulk crystals or molecular clusters instead of the anticipated QDs. It is also important to store the samples at relatively low temperature because at low temperature, it provides strong protection to the core of PbS QDs against the Ostwald ripening which allows us to attain uniform size distribution (Moreels et al. 2009).

STRUCTURAL PROPERTIES

Figure 3 shows the representative HRTEM image of the colloidal PbS QDs prepared in aqueous solution. From the Figure 3, it can be clearly observed that the PbS QDs are closely spherical in shape with monodispersity and clear lattice structure inside the QDs. The QDs size is

approximately 6 ± 1 nm which is smaller than the exciton Bohr radii (18 nm), leading to strong quantum confinement effect by confining the motion of electron and hole. In addition, the QDs are clearly separated from binding together due to protection from the thiols ligands that provide separation distance between QDs. The thiols have high affinity for Pb^{2+} ions and protect the PbS QDs with a steric shielding that screens the Van Der Waals attractions between nearby QDs (Yu et al. 2013).

PHOTOLUMINESCENCE

TEMPERATURE DEPENDENCE OF THE COLLOIDAL PbS QDS PL EMISSION

Figure 4 shows the PL spectra for PbS QDs at a range of T (10 K–300 K). The increment of temperature has several effects on the PL peak energy, PL linewidth and the peak intensity. Based on Figure 4(b), PL peak energy was red-shifted when the temperature is increased from 20 K to 60 K, while it blue-shifted from T >80 K. The energy shifts for temperature higher than 80 K can be described by a temperature coefficient, $\alpha = dE_g/dT = 0.1$ meV/K. This
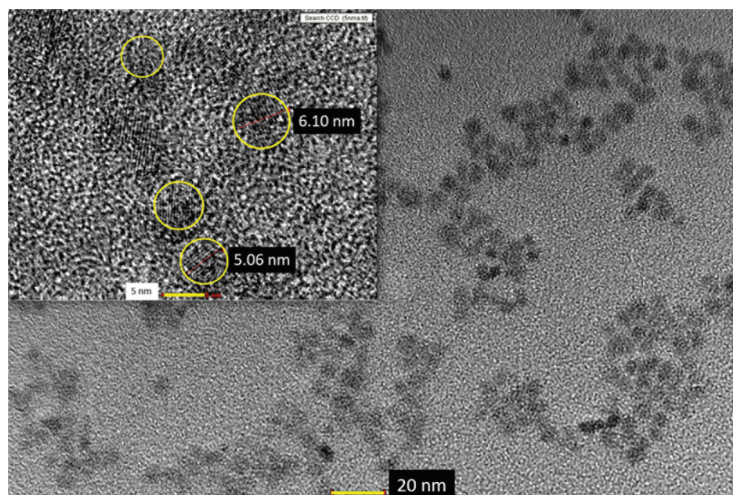
FIGURE 3. HRTEM images of colloidal PbS QDs in aqueous solution

value is smaller compared to bulk PbS ($\alpha = 0.52$ meV/K), but is comparable to that reported in previous study of thiol-capped PbS QDs ($\alpha = 0.3$meV/K) and PbS QDs in glass ($\alpha = 0.2$ meV/K) (Litvyak et al. 2017; Turyanska et al. 2007). Usually, the temperature dependence of the PL peak position can well be described by Varshni equation (Varshni 1967),

$$E_g(\mathrm{T}) = E_g(0) + \alpha \frac{T^2}{\beta + T} \quad (1)$$

where (0) is the band gap at T = 0 K; α represents the band gap energy temperature coefficient; and β is a constant of the order magnitude of the semiconductor material Debye temperature. For this colloidal PbS QDs sample, the second term in (1) with the plus sign (rather than minus sign, as it was in the original equation) was used because the PbS QDs band gap energy increases with the increasing temperature, which is in contrast to most of semiconductor materials.

Commonly, the energy shifts of PL emission with temperature can be caused by some mechanisms. These include thermal expansion of the crystal lattice and electron-phonon coupling (Awschalom & Johnston-Halperin 2001; Wise 2000). When the temperature increases, the distance between atoms in QDs also increases. This will make the energy band gap rises with the increasing temperature as seen in the Figure 4(b) at T > 80 K of our PbS QDs sample. Another dominant contribution to the temperature variation of the energy band gap of the QDs is due to strain between the thermal expansion mismatch and between the QDs and its capping layer (Klotz et al. 2010). These complex mechanisms can lead to a red-shift or blue-shift in the PL peak energy depending on the materials involved. However, Olkhovets et al. (1998) reported that electron-phonon coupling contribution is significantly reduced in the QDs thus produce weaker dependence on temperature of the energy emission in the QD PL emission compared to bulk.

Figure 4(c) shows that the FWHM of the PL signal was also found to be temperature dependent and the linewidth broaden significantly with the increasing temperature for PbS QDs. Unlike isolated atoms, the carriers in the QDs are linked to the vibrational modes of the crystal lattice. The charges that localized in the QDs interact with lattice vibrations via phonons. At low temperature, PL spectrum reflects the distribution of the dot energies because of the charge carriers randomly frozen into the dot states. By increasing the temperature, the interaction between the electron and phonon leads to homogenous broadening of the optical linewidth (Turyanska et al. 2013). Another factor that also affect the PL linewidth is inhomogenous particle size distribution (Fomin et al. 1998). In previous studies of PbS QDs show thermally activated broadening of the linewidth at T ~ 150 K (Turyanska et al. 2007). This thermal activation is also observed for our PbS QDs sample in this research. In addition, the increasing of the FWHM with temperature is explained by the increase in exciton's mobility with temperature (Gruning et al. 2004). As temperature increases, mobility of the excitons also increases, thus resulting in recombination (producing PL) with a broader (nonequilibrium) energy distribution.

Meanwhile, in Figure 4(d), the PL peak intensity shows that the PL intensity reaches maximum at the temperature of 60 K followed by monotonic decrease at T > 80 K. The increase of the PL intensity from 10 K to 60 K indicates that with the increasing T, carriers that are trapped in the defects of the QDs overcome the energy barriers and hence falling down to the QDs ground state. In other words, this is attributed to the thermal excitation of carriers out of QDs defect states followed by carrier relaxation into the ground state. In contrast, the PL intensity shows decreasing trend at the temperature T > 80 K. This quenching of the PL intensity at T > 80 K is associated with the excitation of carriers out of the QDs into non-radiative recombination centers. As temperature increases, the charge carriers gained more energy resulting in recombination of electrons and holes happened rapidly

at a very high rate. This causing intensity to be diluted. Besides that, the quenching of PL emission intensity could partially due to the increasing number of surface defects caused by the ligand displacement (Turyanska et al. 2009).

POWER DEPENDENCE OF PL

Analyzing the dependence of integrated PL (IPL) as a function of excitation power density can provide information of the dominant carrier recombination mechanism (Hasbullah et al. 2009). In Figure 5, the integrated PL across the spectral region (~ 0.7-1.55 eV) is plotted on a log-log scale. Based on their gradients, *m*, the data in Figure 5 can be categorized into three groups, namely, m ~ 1, 1 <*m*< 2, and *m* ~ 2. In this groups, they correspond to the condition where dominant carrier recombination mechanism is radiative (*m* ~ 1), mixture of radiative and nonradiative (associate with defects) (1 <*m*< 2), or nonradiative dominant (*m* ~ 2) (Hasbullah et al. 2009). In other study, Martini et al. (2011) reported that, in a double logarithmic scale, the integrated PL intensity increases linearly with the increasing excitation power density and can be described by the relation,

$$I_{PL} = \eta I_0^{\alpha} \tag{2}$$

where is the integrated PL intensity; and is the excitation power density (Jin et al. 1997). The exponent α depends on the radiative recombination mechanisms and η is the coefficient related to the PL efficiency of the QDs and includes several effects as capture, absorption, ionization and recombination of excitons. As can be seen in Figure 5, the IPL increases linearly with the increasing power density. This similar behavior also can be seen in PbS QDs film and others semiconductor material (Marshall et al. 2016; Ru et al. 2003). However, our sample shows at all temperature measured, the gradient of the graphs is below one and closed to the unity where the radiative recombination is dominant. At 10 K, the slope is 0.69 and at this low temperature, the electron and hole recombine follows radiative recombination path due to excitonic recombination resulting from minimal thermal energy available for exciton dissociation. At 70 K and 150 K, m ~ 0.86 was observed at all excitation power density indicating that radiative recombination is dominant over the entire excitation range investigated. When we increase the temperature to 220 K and 300 K, the slope was increased to 0.91. Papagiorgis et al. (2016) also reported almost similar result where the slope for their PbS QDs solid is m ~ 0.96 above 200 K which exhibits a monomolecular behavior up to moderate excitation powers.
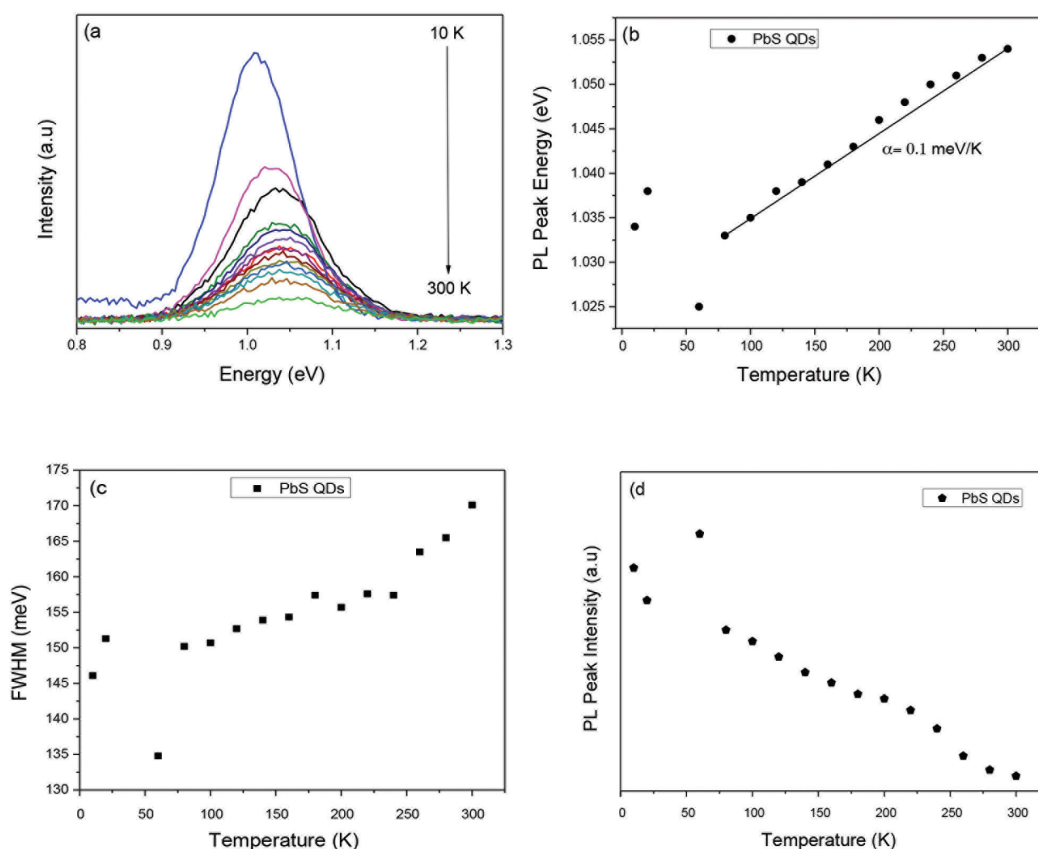

FIGURE 4. Temperature dependence of the PL properties for colloidal PbS QDs showing the PL peak energy, the FWHM and the PL intensity
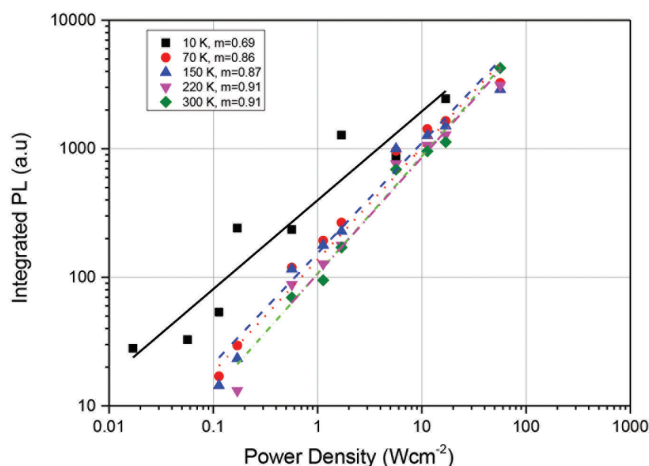
FIGURE 5. Integrated PL intensity (IPL) versus excitation power
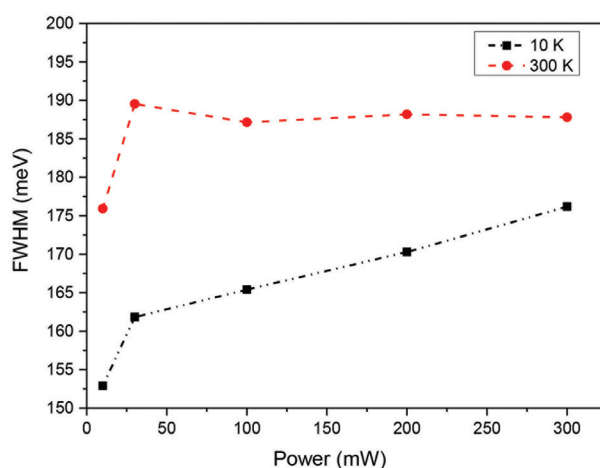density at different temperatures for PbS QDs

FIGURE 6. FWHM of PbS QDs at different power excitation at 10 K and 300 K

Figure 6 shows the FWHM of the sample at different power excitation at low temperature (10 K) and at the room temperature (300 K). As can be seen in the Figure 6, the FWHM of the sample at 300 K are higher than at 10 K at all particular power excitation measured. As described previously, at higher temperature, the charge carriers become more mobile, thus broaden the PL linewidth with a nonequilibrium energy distribution. Furthermore, as the power excitation increases, the FWHM also increases for both temperatures (at 10 K and 300 K). This behavior is due to band filling effect where it happens by occupying the low energy states of energy bands by the particles.

CONCLUSION

In summary, colloidal PbS QDs capped with thiol ligands in aqueous solution was synthesized with stable photoluminescence in the near IR spectral range and the effect of temperature and power excitation towards the PL of PbS QDs was studied at the temperature range from 10 K to 300 K. The PL peak energy, PL peak intensity

and FWHM of the sample are temperature dependent. Intensity of the PL increased at low temperature (10 K - 60 K). On the other hand, the intensity dropped when the temperature above 80 K due to activation of non-radiative recombination. We have observed a thermally activated increase the FWHM of our sample and explained this behavior in terms of the interaction between charge carriers and phonons at high temperature. We also found that the energy band gap of QDs is due to the size of QDs that related to quantum confinement effect. Recombination mechanism of charge carriers can be clearly observed by the measurement of power dependent towards PL emission.

REFERENCES

Alivisatos, A.P. 1996. Semiconductor clusters, nanocrystals, and quantum dot. *Science* 271(5251): 933-937.

Ashari, F., Liew, J.Y.C., Talib, Z.A., Yunus, W.M.M., Jian, L., Kee, L., Dee, C. & Yeop Majlis, B. 2016. Optical characterization of colloidal zinc selenide quantum dots prepared through hydrothermal method. *Sains Malaysiana* 45(8): 1191-1196.

Awschalom, D.D. & Johnston-Halperin, E. 2001. Spin spectroscopy of dark excitons in CdSe quantum dots to 60 T. *Physical Review B* 63: 1-5.

Binetti, E., Striccoli, M., Sibillano, T., Giannini, C., Brescia, R., Falqui, A. & Comparelli, R. 2015. Tuning light emission of PbS nanocrystals from infrared to visible range by cation exchange. *Science and Technology of Advanced Materials* 16(5): 1-10.

Fomin, V.M., Gladilin, V.N., Devreese, J.T., Pokatilov, E.P., Balaban, S.N. & Klimin, S.N. 1998. Photoluminescence of spherical quantum dots. *Physical Review B* 57(4): 2415-2425.

Gao, F. 2011. Effects of quantum confinement and shape on band gap of core/shell quantum dots and nanowires. *Applied Physics Letter* 98(193105): 3-6.

Gruning, H., Kohary, K., Baranovskii, S.D., Rubel, O., Klar, P.J. & Ramakrishnan, A. 2004. Hopping relaxation of excitons in GaInNAs/GaNAs quantum wells. *Physics States Solid* 112(1): 109-112.

Guchhait, A., Rath, A.K. & Pal, A.J. 2011. To make polymer: Quantum dot hybrid solar cells NIR-active by increasing diameter of PbS nanoparticles. *Solar Energy Materials and Solar Cells* 95(2): 651-656.

Hasbullah, N.F., Ng, J.S., Liu, H., Hopkinson, M., David, J.P.R., Badcock, T.J. & Mowbray, D.J. 2009. Dependence of the electroluminescence on the spacer layer growth temperature of multilayer quantum-dot laser structures. *IEEE Journal of Quantum Electronics* 45(1): 79-85.

Iacovo, A., Venettacci, C., Colace, L., Scopa, L. & Foglia, S. 2016. PbS colloidal quantum dot photodetectors operating in the near infrared. *Nature Publishing Group* 6: 1-9.

Jin, S., Zheng, Y., Li, A., Jin, S., Zheng, Y. & Li, A. 1997. Characterization of photoluminescence intensity and efficiency of free excitons in semiconductor quantum well structures. *Journal Applied Physics* 82(8): 3870-3873.

Klotz, F., Jovanov, V., Kierig, J., Clark, E.C., Rudolph, D., Heiss, D. & Bichler, M. 2010. Observation of an electrically tunable exciton gfactor in InGaAs/GaAs quantum dots. *Applied Physics Letter* 96: 053113.

Litvyak, V.M., Cherbunin, R.V. & Onushchenko, A.A. 2017. Temperature dependence of the optical transitions of PbS quantum dots in silicate glasses. *Bulletin of the Russian Academy of Sciences: Physics* 81(12): 1490-1492.

Liu, Y., Kim, D., Morris, O.P., Zhitomirsky, D. & Grossman, C. 2018. Origins of the Stokes shift in PbS quantum dots. *ACS Nano* 12: 2838-2845.

Marshall, A.R., Beard, M.C. & Johnson, J.C. 2016. Nongeminate radiative recombination of free charges in cation-exchanged PbS quantum dot films. *Chemical Physics* 471: 75-80.

Martini, S., Teles, L.K., Marques, M., Marques, A.E.B. & Quivy, A.A. 2011. Radiative recombination mechanisms of large InAs/GaAs quantum dots. *World Journal of Condensed Matter Physics* 1: 161-166.

Moreels, I., Lambert, K., Smeets, D., Muynck, D.D., Nollet, T., Martins, C., Vanhaecke, F., Delerue, C., Allan, G. & Hens, Z. 2009. Size-dependent optical properties of colloidal PbS quantum dots. *ACS Nano* 3(10): 3023-3030.

Okamoto, K., Niki, I., Shvartser, A., Narukawa, Y., Mukai, T. & Scherer, A. 2004. Surface-plasmon-enhanced light emitters based on InGaN quantum wells. *Nature Publishing Group* 3: 601-605.

Olkhovets, A., Hsu, R., Lipovskii, A. & Wise, F.W. 1998. Size-dependent temperature variation of the energy gap in lead-salt quantum dots. *Physical Review L* 81(16): 3539-3542.

Papagiorgis, P., Stavrinadis, A., Othonos, A., Konstantatos, G. & Itskos, G. 2016. The influence of doping on the optoelectronic properties of PbS colloidal quantum dot solids. *Nature Publishing Group* 6(18735): 1-16.

Peterson, J.J. & Krauss, T.D. 2006. Fluorescence spectroscopy of single lead sulfide quantum dots. *Nano Letters* 6(3): 510-514.

Rajh, T., Olga, I., Micic, O.I. & Nozik, A.J. 1993. Synthesis and characterization of surface-modified colloidal CdTe quantum dots. *The Journal of Physical Chemistry* 97(46): 11999.

Reilly, N., Wehrung, M., O'Dell, R.A. & Sun, L. 2014. Ultrasmall colloidal PbS quantum dots. *Materials Chemistry and Physics* 147: 1-4.

Rogach, A.L., Eychmüller, A., Hickey, S.G. & Kershaw, S.V. 2007. Reviews infrared-emitting colloidal nanocrystals: Synthesis, assembly, spectroscopy, and applications. *Small Journal* 4: 536-557.

Ru, E.C.L., Fack, J. & Murray, R. 2003. Temperature and excitation density dependence of the photoluminescence from annealed InAs/GaAs quantum dots. *Physical Review B* 67: 245318.

Ryu, S., Park, J., Oh, J., Long, D.H., Kwon, K., Kim, Y., Lee, J.K. & Kim, J.H. 2009. Analysis of improved efficiency of InGaN light-emitting diode with bottom photonic crystal fabricated by anodized aluminum oxide. *Advanced Functional Materials* 19: 1650-1655.

Sargent, E.H. 2005. Infrared quantum dots. *Advanced Materials* 17(5): 515-522.

Shamsudin, S. & Junas, J. 2018. Kajian terhadap sifat optik titik kuantum kadmium sulfida pada pelbagai nilai pH dan modifikasi permukaan dengan asid tioglikolik. *Sains Malaysiana* 47(11): 2841-2849.

Szendrei, K., Speirs, M., Gomulya, W., Jarzab, D., Manca, M., Mikhnenko, O.V., Yarema, M., Kooi, B.J., Heiss, W. & Loi, M.A. 2012. Exploring the origin of the temperature-dependent behavior of PbS nanocrystal thin films and solar cells. *Advanced Functional Materials* 22: 1598-1605.

Tasco, V., Baranov, A. & Satpati, B. 2007. Molecular-beam epitaxy of InSb/GaSb quantum dots. *Journal of Applied Physics* 101: 124309.

Turyanska, L., Moro, F., Knott, A.N., Fay, M.W., Bradshaw, T.D. & Patanè, A. 2013. Paramagnetic, near-infrared fluorescent Mn-doped PbS colloidal nanocrystals. *Particle & Particle Systems Characterization* 30: 945-949.

Turyanska, L., Elfurawi, U., Li, M., Fay, M.W. & Thomas, N.R. 2009. Tailoring the physical properties of thiol-capped PbS quantum dots by thermal annealing. *Nanotechnology* 20: 315604.

Turyanska, L., Patanè, A. & Henini, M. 2007. Temperature dependence of the photoluminescence emission from thiol-capped PbS quantum dots. *Applied Physics Letter* 90: 101913.

Varshni, P. 1967. Temperature dependence of the energy gap in semiconductors. *Physica* 34: 149-154.

Wang, J.S., Smith, H.E. & Brown, G.J. 2015. Stability and aging studies of lead sulfide quantum dot film: Photoabsorption, morphology, and chemical state characteristics. *Materials Chemistry and Physics* 154: 44-52.

Wise, F.W. 2000. Lead salt quantum dots: The limit of strong quantum confinement. *Accounts of Chemical Research* 33(11): 773-780.

Yamada, Y., Yasuda, H., Tayagaki, T. & Kanemitsu, Y. 2009. Temperature dependence of photoluminescence spectra of non-doped and electron-doped SrTiO 3: Crossover from Auger recombination to single-carrier trapping. *Physical Review Letter* 102: 247401.

Yang, L.M., Ye, Z.Z., Zeng, Y.J., Xu, W.Z., Zhu, L.P. & Zhao, B.H. 2006. Density controllable growth of ZnO quantum dots by MOCVD. *Solid State Communications* 138: 577-579.

Yin, Y. & Alivisatos, A.P. 2005. Colloidal nanocrystal synthesis and the organic-inorganic interface. *Nature* 437: 664-670.

Yoffe, A.D. 2001. Semiconductor quantum dots and related systems: Electronic, optical, luminescence and related properties of low dimensional systems. *Advances in Physics* 50(1): 1-208.

Yu, Y., Zhang, K. & Sun, S. 2013. Effect of ligands on the photoluminescence properties of water-soluble PbS quantum dots. *Journal of Molecular Structure* 1031: 194-200.

Zhou, S., Liu, Z., Wang, Y., Lu, K., Yang, F., Gu, M., Xu, Y., Chen, S., Ling, X., Zhang, Y., Li, F., Yuan, J. & Ma, W. 2019. Towards scalable synthesis of high-quality PbS colloidal quantum dots for photovoltaic applications. *Journal of Materials Chemistry C* 7: 1575-1583.

Muhammad Safwan Zaini, Mazliana Ahmad Kamarudin & Josephine Liew Ying Chyi
Department of Physics
Faculty of Science
Universiti Putra Malaysia
43400 UPM Serdang, Selangor Darul Ehsan
Malaysia

Shahrul Ainliah Alang Ahmad
Department of Chemistry
Faculty of Science
Universiti Putra Malaysia
43400 UPM Serdang, Selangor Darul Ehsan
Malaysia

Abdul Rahman Mohmad
Institute of Microengineering and Nanoelectronics
Level 4, Research Complex
Universiti Kebangsaan Malaysia
43600 UKM Bangi, Selangor Darul Ehsan
Malaysia

*Corresponding author; email: mazliana_ak@upm.edu.my